

In-Flight Identification of the Galileo Spacecraft Flexible Mode Characteristics

Edward C. Wong*

Jet Propulsion Laboratory, California Institute of Technology, Pasadena, California

The scan platform of the Galileo spacecraft is attached to a flexible stator structure that separates the actuator from the platform-mounted inertial sensor. A scheme to identify the flexible mode characteristics (frequency, damping, and modal coefficient) of the stator using flight data is presented. A frequency domain analysis approach is taken and the identified mode characteristics will be used for updating the scan platform controller parameters. The influence of structural flexibility to the scan controller design is explained and the constraints in executing the identification procedure in flight are discussed. Computer simulation results of the identification scheme are presented. The scheme is further verified by DISCOS simulations, in conjunction with a full spacecraft dynamics model and the scan platform controller.

Introduction

THE Galileo project is a planetary mission to Jupiter scheduled for launch in 1986. The dual-spin configured spacecraft will orbit Jupiter to conduct scientific investigation of the planet and its satellites. A probe will be released prior to Jupiter orbit insertion and will follow an impact trajectory for atmospheric investigation.^{1,2} A sketch of the Galileo spacecraft is shown in Fig. 1. There are two degrees of freedom for controlling the scan platform's inertial orientation. A clock actuator controls the relative position between the rotor (spinning portion) and the stator (nonspinning portion), and a cone actuator controls the relative position between the platform and the stator. These two actuators control the clock and cone axis, which are perpendicular to one another so that the platform may be gimballed in two orthogonal directions.

The influence of flexible body dynamics is crucial for the design and performance of the Galileo's platform pointing system. Instruments such as the solid-state imaging camera and the near-infrared mapping spectrometer are mounted on the scan platform connected to the flexible stator. These instruments are the primary cause of stringent pointing (62.5 μ rad) and stability (20 μ rad per 1 s exposure) requirements for Galileo.

Uncertainty remains, however, as to where exactly these undesirable frequencies are. Prelaunch measurement data of the structure suggest that a miss in the destabilizing frequencies may be within $\pm 20\%$, and that a discrepancy between ground-predicted and actual mode shape and frequencies up to $\pm 50\%$ is quite likely. Therefore, there is a need for an in-flight identification of the flexible mode characteristics below 15 Hz to enhance the performance of the notch filter and stabilize the platform motion.³

Structural Flexibility

and Controller Design Considerations

The stator structure to which the platform is attached is quite flexible. It has six very lightly damped natural frequencies below 15 Hz. Furthermore, the clock actuator is separated from the gyros by the flexible stator. Evaluation of the structural data indicates that the stator structural modes that are of greatest impact to the platform controller exist in the range of 2.5-15 Hz. These frequencies are near the controller bandwidth (around 1 Hz). In order to prevent the flexible motion from feeding back into the structure through the clock actuator, a wide notch filter is implemented in the platform controller.

Scan Controller Design

The scan pointing algorithms in clock axis include a scan commander, a proportional-integral-derivative controller, a notch filter, and a torque summing junction. Upon receiving the attitude knowledge of the scan platform, the scan commander processes pointing commands to determine the target position of the scan platform and the slew path required to reach that position. It also generates feedback position and rate errors for the scan controllers in both clock and cone axes.⁴ The clock actuator is also referred to as the spin bearing assembly (SBA) actuator and the cone actuator as the scan articulation subsystem (SAS) actuator.

The cone actuator and the gyros are separated by a rigid platform structure and, therefore, gyro measurement can be used directly in the control about the cone axis by the cone actuator. However, the clock actuator is separated from the gyros by the stator structure, which is flexible in nature. Due to this noncollocation of actuator and sensor for the clock control loop, the gyro data contain information on the flexible motion of the scan platform as well as the rigid-body motion. When the flexible motion is fed back into the structure through the clock actuator, e.g., when the controller is attempting to compensate a position error due to flexible vibration at a resonance frequency, it may destabilize the control loop. Another undesirable phenomenon is that the platform may move in an opposite direction to the control torque before reversing its direction and following the commanded direction. This is known as a nonminimum phase behavior and is exhibited by low-frequency modes.

The effect of flexibility on stability can be observed from an open-loop Bode plot of the stator structure in clock control loop (Fig. 2). The modes at resonance frequencies of 8.4 and

Presented as Paper 84-1965 at the AIAA Guidance and Control Conference, Seattle, WA, Aug. 20-22, 1984; submitted Oct. 15, 1984; revision received June 21, 1985. Copyright © American Institute of Aeronautics and Astronautics, Inc., 1985. All rights reserved.

*Member of Technical Staff, Guidance and Control Section. Member AIAA.

9.3 Hz have high resonance peaks and may very likely cause instability once the loop is closed.

Notch Filter

An approach taken in the Galileo's scan controller design to stabilize the pointing system is to add a notch filter: a filter to greatly attenuate the control system gain at the notch frequency. The purpose is to use the filter to reduce the resonance peaks in magnitude to levels having reasonable stability margins. The use of the notch filter is briefly described in the following paragraphs.

The transfer function of the notch filter used in Galileo's scan controller's design (in the s domain) takes the form

$$\frac{\text{Output (s)}}{\text{Input (s)}} = \left(\frac{s^2 + \lambda^2}{s^2 + 2\zeta_n \lambda s + \lambda^2} \right)^2 \quad (1)$$

where λ is the resonance frequency that is to be notched out. The value for ζ_n varies between 0 and 1, with 0 being a narrow notch and 1 being the widest notch. If the knowledge of the resonance frequency is less certain, a wide notch is desired, which effectively widens the frequency range for gain attenuation. Equation (1) shows two cascaded notches, or a "double-notch" filter, which provides essentially double the attenuation as a single notch.

The double-notch filter in Eq. (1) is converted to a z transfer function using the pole/zero mapping method and is implemented for Galileo's digital controller as follows:

$$\frac{\text{Output (z)}}{\text{Input (z)}} = \left[\frac{(z - e^{-j\lambda T})(z - e^{j\lambda T})}{(z - e^{-\lambda T})^2} \right]^2 \quad (2)$$

where T is the digital sampling period. When the structural frequency has a large resonance peak, the notch frequency λ will be set exactly at that frequency to achieve maximum attenuation. However, if the structure has a number of modal frequencies with large resonance peaks, then rather than picking one of these frequencies to be notched, we may use the notch filter more as a low pass or rolloff filter. That is, the filter attenuates frequencies higher than the notch frequency, but pass the lower frequencies with little or no attenuation. However, caution must be taken not to notch the lower frequencies by a wide notch filter as this may reduce the controller bandwidth and degrade the platform's pointing performance.

The purpose of designing an in-flight identification of the structural resonance frequencies is to locate the "destabilizing frequencies" (to within 5%) and the corresponding mode shape (to within 20%) so as to determine the proper parameter values for the notch filter. Once the flexible mode characteristics are determined, the filter parameters stored in the onboard flight software will be updated.

Structural Flexibility Sensed by Platform-Mounted Gyros

The Galileo spacecraft configuration showing the relationship between the stator (X, Y, Z) and platform (M, N, L) coordinates is shown in Fig. 1. The scan pointing performance is measured by the pointing accuracy of the instrument boresight vector (along the L axis). This pointing error is computed by the scan commander in terms of the position and rate error information about the platform cone N and cross-cone M axes. Motions about these two axes can be sensed by the gyros. Note that N is aligned with Y and that the L, M, X, Z axes all lie on the same plane. The L axis may be oriented by varying the cone angle β , where $0 \leq \beta \leq 210$ deg.

As seen in Fig. 1, any flexibility motion about the stator Y will fully appear along the platform N axis. The error about the N axis is controlled by the cone controller. As mentioned earlier, structural flexibility is not a problem for the cone con-

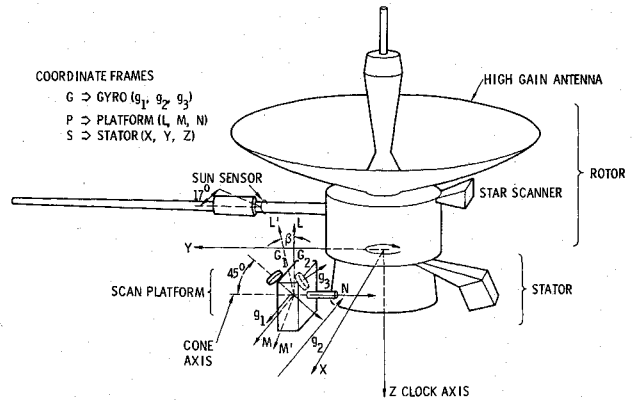


Fig. 1 Galileo spacecraft stator and platform coordinate systems.

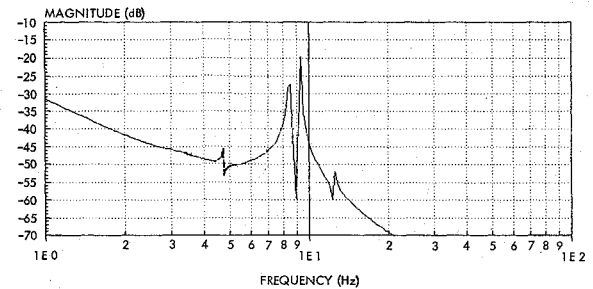


Fig. 2 DISCOS generated clock loop structural response (cone at 90 deg).

trol loop since the sensor and actuator are collocated. On the other hand, there is a variation in the observability of flexibility components in the stator X and Z by the gyros as the cone angle β varies. This has a significant impact to the clock controller, which controls the clock motion based on the error observed by the gyros along the M axis. M is aligned with X when $\beta = 0$. Components in Z rather than in X is more observable along the platform M axis for β close to 90 deg and in X rather than Z for β near 0 or 180 deg. For example, at a cone angle of $\beta = 90$ deg, M is directly along Z and, hence, observes all of the flexible motion components about Z and none of the X components. The ratio of the observability in flexibility components of $X(F_x)$ to $Z(F_z)$ along the platform M axis is given by

$$F_x/F_z = \cot(\beta) \quad (3)$$

Within the region of $170 \leq \beta \leq 190$ deg, no M axis measurements will be used for scan control because of the existence of singularity at $\beta = 180$ deg. Note that when β is near 170 deg, the ratio in Eq. (3) approaches 5.6. That is, at this cone angle, the flexibility motion in X is approximately five times more visible to the clock control loop than the motion in Z .

Constraints on In-Flight Identification

There are several hardware and system limitations that affect the design of an in-flight identification method on flexible mode characteristics. They are briefly outlined in this section.

Actuator and Sensor Characteristics

Besides the noncollocation of the actuator (clock) and the sensor (gyros), there are limits in both the actuator's torque level and the sensor data rate for telemetry. The actuator torque saturates at around 4 N·m. The ability of discerning the platform vibrations for accurate identification of the mode characteristics depends, to a large extent, on the sufficiency of torque (or energy) applied to excite the structure. The rate-

integrating gyros have a rolloff frequency at about 15 Hz, saturate at a capture rate of 3 deg/s, and their measurements are quantized at $5.99 \pm 5\% \mu\text{rad}$. Furthermore, the highest telemetry rate in Galileo is 15 Hz (66 2/3 ms rate group) and is limited to transmitting a maximum of six variables.

Onboard Computer Memory and Software Constraint

Galileo's attitude control onboard computer has a total memory of 32 K. At the time of this design, the memory margin is extremely tight. The total onboard memory usage for the in-flight identification process must be strictly minimized. Furthermore, most of the flight software design has been coded and is currently undergoing an extensive testing phase. Any changes requested by the identification process shall minimally impact the existing flight software. For example, the type of torque input (e.g., step, ramp, sinusoidal, etc.) required to be generated should be compatible to the existing control system software design.

Onboard Fault Protection

One of the challenges of the present identification design is to obtain an open-loop response of the stator/platform system while maintaining a "closed-loop" capability in the event of an anomaly during the identification process. The structure should be excited to a level within the fault limits set by onboard fault protection logic. Also, the design should be carefully correlated with fault protection to ensure an automatic and immediate abort of the process in the event that any fault is detected.

Identification Strategy

The basic approach in the identification of the stator flexible mode characteristics is to first establish a ground-based dynamical model of the rotor/stator structure in the clock control loop that includes all of the characteristics (modal coefficients, frequencies, and damping) of the expected flexible modes under 15 Hz. The model consists of a transfer function of n flexible modes in the form

$$T(j\omega) = \sum_{j=1}^N \frac{c_j}{(j\omega)^2 + 2\zeta_j\lambda_j(j\omega) + \lambda_j^2}, \quad j = \sqrt{-1} \quad (4)$$

where c_j is a modal coefficient, ω a frequency variable in rad/s, ζ_j a modal damping factor, and λ_j the modal or resonance frequency in rad/s. Parameters λ_j , c_j , and ζ_j for $j = 1, \dots, N$ are the unknown flexible mode characteristics to be identified and N is the number of modes with resonance frequency below the gyro rolloff frequency (15 Hz). A power spectral density (PSD) analysis approach is taken to identify the mode characteristics by exciting the flexible stator structure using an applied SBA (clock actuator) torque.

The modal frequencies are first determined by analyzing the PSD of the gyro telemetry data measuring the stator response. Both the modal coefficients and the damping factor of each mode are then adjusted such that the model can reproduce the same spectrum as the one produced from telemetry data, in frequency and amplitude, to some satisfactory accuracy. Note that the model should use an identical torque input (e.g., pulse width) as one used in flight.

Frequency Domain Analysis

The PSD analysis chosen in this study uses an algorithm that employs the Fast Fourier Transform (FFT) to calculate the PSD of the gyro output variable $\Delta\theta(t)$. This is done by first estimating the autocovariance function of the variable,

$$R(\tau) = E[\Delta\theta(t)\Delta\theta(t+\tau)^T] \quad (5)$$

where E is the statistical expectation operator. Then the power density spectrum $S(\omega)$ is obtained by taking the FFT of the

smoothed autocovariance function,

$$S(\omega) = \int_{-\infty}^{\infty} e^{-j\omega\tau} R(\tau) d\tau \quad (6)$$

The current identification design uses a computer program for computing the PSD as given in Ref. 5. This program works with both continuous and discrete data.

The phase information can be extracted from the ratio of the gyro output FFT to the torque input FFT at each modal frequency. The resulting phase angles corresponding to these ratios indicate the relative phase lags of the flexible modes at the starting time of the gyro measurements.

The shape of the PSD centered at a modal frequency is a function of the modal coefficient c and damping factor ζ . The relation can be easily described by considering a structural response (e.g., due to a square torque pulse) to be a damped sinusoidal function of the form,

$$f(t) = ce^{-\zeta\lambda t} \sin\lambda t \quad (7)$$

where λ is the resonance frequency. The Fourier transform of $f(t)$ is approximately

$$g(\omega) \approx -\frac{c}{2} \left[\frac{1}{\omega - \lambda - i\zeta\lambda} \right] \quad (8)$$

for frequency $\omega \approx \lambda$ and $\zeta \ll 1$. (Values of ζ are typically below 0.01.) The PSD of $f(t)$ is $|g(\omega)|^2$, which is proportional to

$$|g(\omega)|^2 \propto \frac{c^2}{(\omega - \lambda)^2 + (\zeta\lambda)^2} \quad (9)$$

It is clear that c^2 affects the magnitude of $|g(\omega)|^2$ proportionally, while the magnitude (height) of $|g(\omega)|^2$ is only sensitive to the variation of ζ when the frequency is near λ . However, $|g(\omega)|^2$ becomes rather insensitive to ζ when ω moves away from λ , since $(\zeta\lambda)^2$ will become negligible compared to $(\omega - \lambda)^2$.

Input Torque

The input to the clock control loop is the torque generated from the SBA. Hence, the SBA is selected to be the source of torque input to excite the spacecraft flexible structure.

A torque pulse is chosen because it is easy to implement and resembles a torque impulse. Its frequency harmonics content enables the excitation of flexible modes over a larger frequency range of interest. However, the SBA torquer saturates at 4 N·m. The only alternative to increasing torque magnitude is to increase the torquing duration such that enough energy can be imparted to the system to excite the flexible modes.

Pulse Width Variability

A torque square pulse exhibits various frequency harmonics whose nodes are a function of the pulse width Δt , located at $n/\Delta t$ Hz, $n = 1, 2, 3, 4, \dots$ (Fig. 3). The PSD of a square pulse of width Δt is a function of the frequency ν in Hertz,⁶

$$S(\nu) = \frac{\sin^2(\pi\nu\Delta t)}{(\pi\nu)^2\Delta t} \quad (10)$$

The PSD in Eq. (10) indicates that a square pulse would excite the lower-frequency modes more than the higher ones. Because of this frequency harmonics characteristic, the flexible modes located within approximately ± 0.1 Hz from each node will not be adequately excited (determined by computer simulation results). Therefore, it is essential to design an identification scheme that is able to generate torque pulses with variable pulse widths, such that all the frequencies within the range of interest should be at least 0.1 Hz away from at least one node.

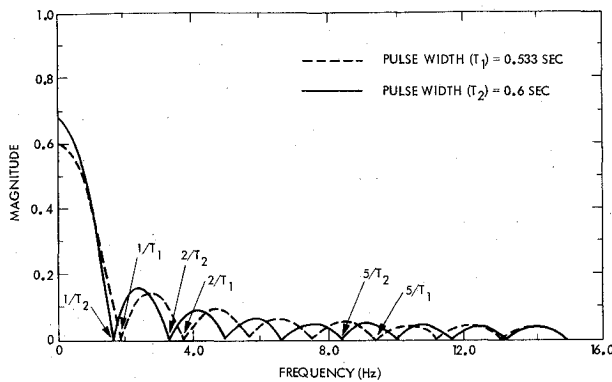


Fig. 3 Power spectral density of square pulses.

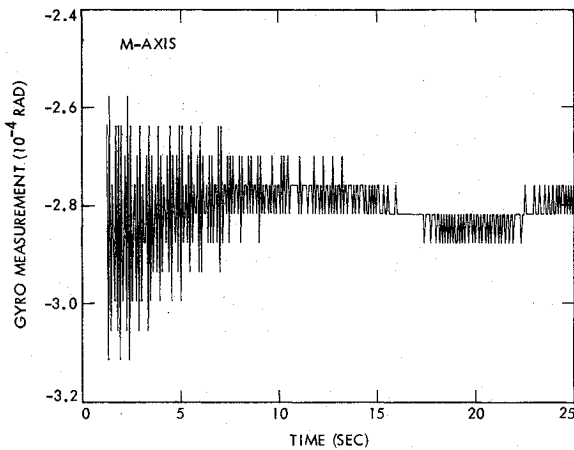


Fig. 4 Gyro telemetry data of stator vibrational response.

The real-time interrupts designed for Galileo's attitude control flight software can provide a variability of a torque pulse width to a resolution of $66\frac{2}{3}$ ms. The $66\frac{2}{3}$ ms is the interval between attitude control flight software real-time interrupts (RTI). Most of the attitude determination and control functions are executed once in this interval. Ten RTI intervals constitute a "minor frame" for telemetry. The current identification design requires specifying a certain RTI interval of a minor frame in which real-time commands are to be executed. This new capability enables variability in the pulse width that depends on the interval between the servicing of two commands. Furthermore, this change also provides flexibility in the command servicing time and better predictability in the subsystem response to command executions.

Telemetry Data

A special mode for telemetry, known as the "flood mode," has been created for the purpose of in-flight identifications. The flood-mode telemetry buffer provides up to six measurements of telemetry variables at a rate of $66\frac{2}{3}$ ms. Normally, the flood-mode telemetry buffer is not part of the regular telemetry stream. To obtain the telemetry data in this mode, the buffer must be transferred to a command data subsystem (CDS) bulk memory once every $\frac{2}{3}$ s and then read out for that memory. Each memory readout from the bulk memory contains a maximum of 28 s of sampling at 15 samples/s, or a total of 420 pieces of sampled data per telemetry variable.

Gyro Data Processing

Gyro data are the only sensor data that provide adequate resolutions in sensing the platform's rate and position. Because the clock control loop uses only the *M* axis measure-

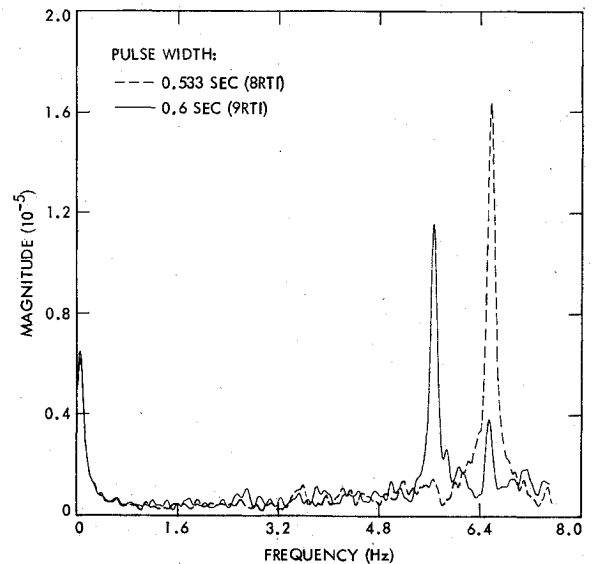


Fig. 5 Power spectral density of stator vibrational data.

ment, we let $\Delta\theta$ be the gyro data along that axis. Position information measured by the gyro is given by

$$\theta(t_{k+1}) = \theta(t_k) + \Delta\theta(t_k, t_{k+1}) \quad (11)$$

where $t_k, t_{k+1}, t_{k+2} \dots$ are the gyro sampled times and (t_k, t_{k+1}) indicates a time interval. Also, the rate information $\dot{\omega}(t)$ provided by the gyros is given by

$$\dot{\omega}(t_k, t_{k+1}) = \frac{\Delta\theta(t_k, t_{k+1})}{t_{k+1} - t_k}, \quad k = 0, 1, 2, \dots \quad (12)$$

In the execution of Galileo's flight software, $(t_{k+1} - t_k)$ is constant for all values of k in the period that the gyro samples are collected; therefore, we can simply use the $\Delta\theta(t_k, t_{k+1})$ data directly as a rate data

Friction Compensation

When the spacecraft is in the dual-spin configuration, the SBA slip ring produces a friction that tends to spin up the stator in the same direction as the rotor spin direction (positive motion about *Z*). After the torque pulse is initiated, the data for identification result can be best obtained when no other torque, including frictional torque, will be acting on the stator. This will prevent additional excitation of the flexible modes after the torque pulse is generated. The amount of friction can be estimated by simply observing from telemetry the SBA torque bias needed to keep the stator despin (at 0 rate) prior to the identification process. The observation error will be down to the torque resolution (4×10^{-3} N·m). Friction can be "cancelled" by commanding a fixed-bias torque negatively about *Z*. Although ground test data have characterized that the SBA friction is fairly constant at constant encoder rates, it is impossible to totally cancel the frictional torque this way due to the existence of low-level frictional noise of random characteristics.

Flight Implementation

The in-flight identification process is to be executed by ground commands timed accurately within $66\frac{2}{3}$ ms (the rate group for scan control) to generate torque pulses by the clock actuator. Two types of commands are required to generate a torque pulse: a 7SLEW and a 7DBSE (data base) command. The 7SLEW commands the stator to slew at a specified rate relative to the rotor, that is, at a specified encoder derived rate. Unlike other science and imaging scan commands, which

Table 1 Command sequence for state or flexible mode identification

Time	Command
T	Command (7 SLEW) to despin the stator to 0 deg/s Command to a cone angle β
$T + 10 \text{ min}$	Command (7DBSE) to specify a desired real-time interrupt for the subsequent 7 DBSE command (to vary pulse width of torque applied)
$T + 10 \text{ min} + \frac{2}{3} \text{ s}$	Command (7 SLEW) to spin up the stator to -1 deg/s
$T + 10 \text{ min} + 1 \frac{1}{3} \text{ s}$	Command (7 DBSE) to lower the SBA torque saturation limit to be the same as the "observed" steady-state friction
$T + 10 \text{ min} + 30 \text{ s}$	Command (7 DBSE) to restore the SBA torque saturation limit to nominal value
$T + 10 \text{ min} + 30 \frac{2}{3} \text{ s}$	Repeat last 7DBSE command

normally follow a smooth, open-loop torque profile to avoid exciting the flexible stator structure, the 7SLEW command would initiate a control torque almost instantaneously and does not follow any torque profile. The 7DBSE command is used to update the flight software parameters stored in the data base. These two commands would enable the SBA to generate a torque pulse at a specified pulse width down to 66⅔ ms accuracy.

The torque generated by the SBA is inherently constrained by power supply. Saturation arises when torque is requested to go beyond a hardware limit. The attitude control flight software, on the other hand, sets a software limit that is slightly below the hardware limit. The controller torque and the open-loop feedforward torque (if any) are totaled. The resulting torque information is passed through an encoder hardware interface program to request for a desired SBA torque. The requested torque will then be limited by a saturation level that is defined as a software parameter.

A torque pulse can be generated by the following procedure: the stator is initially despun (inertially stationary). Then it is commanded by a 7SLEW to slew at a high rate (-1 deg/s) that would instantly saturate the SBA software torque limiter. Then, a 7DBSE command is sent and will be serviced at a specified time to lower the saturation level and to bring the command torque limit to a level just enough to "cancel" the steady-state friction. The instantaneous change of the command torque limit generates a discontinuity that resembles a torque pulse. The lower torque limit is maintained for a time period ($\sim 27 \text{ s}$), while gyro data are continuously sampled at 66⅔ ms interval. Until the torque limit is restored to its nominal level, the clock controller remains essentially in a state of an open loop.

The command sequence shown in Table 1 represents an in-flight procedure for the stator flexible mode identification. Except for the essential attitude determination and control maintenance, no attitude control maneuvers that require thruster pulsing (such as spin rate control, high-gain antenna pointing control, etc.) should be active during the identification process. The SBA torque in dual-spin mode has to be recorded from telemetry prior to these commands in order to determine the steady-state SBA friction.

The time interval between the second 7SLEW and the second 7DBSE command may be 0, $\frac{2}{3} \text{ s}$ or $1 \frac{1}{3} \text{ s}$ depending on the size of pulse width to be generated. The identification procedure will be performed for at least four different pulse widths in order to cover all frequencies in the frequency spectrum below 15 Hz. Then the process will be repeated for various cone angles, possibly 90-170 deg at increments of 20 deg. The last 7DBSE command is sent to ensure that the command torque limit will be restored to the normal level.

Table 2 Modal frequencies and coefficients for simulations

Cone angle β , deg	Flexible mode	Modal frequency $\lambda/2\pi$, (Hz)	Modal coefficient c_i	Modal damping ζ_i , %
90	1	3.16	7.994×10^{-7}	0.75
	2	4.60	-3.714×10^{-4}	2.74
	3	6.81	1.015×10^{-5}	0.65
	4	8.43	-6.594×10^{-3}	0.34
	5	9.31	-5.966×10^{-3}	0.23
	6	12.49	-2.853×10^{-3}	0.72
170	1	2.56	-0.286×10^{-3}	0.25
	2	4.43	1.306×10^{-3}	0.25
	3	6.47	-1.525×10^{-3}	0.25
	4	7.55	-5.303×10^{-3}	0.25
	5	8.76	3.425×10^{-3}	0.25
	6	12.67	-1.146×10^{-3}	0.25

Design Verification by Computer Simulations

To verify the validity and performance of the identification scheme, a comprehensive and reasonably accurate dynamical model is essential. Short of the actual spacecraft flight data, a full-blown simulation of the spacecraft dynamics and scan controller using the DISCOS program⁷ appears to provide the best available data for design verification. Two different models are being used for the current study: a simpler, one-dimensional dynamics model of the Galileo spacecraft (along one axis) and a four-body (platform, stator, rotor, and magnetometer boom) DISCOS program that models the spacecraft in three axes and including such characteristics as the dynamical coupling and rotational dynamical effects. The simpler model was used for extensive simulation runs, while the DISCOS program was used to compare and validate the simpler model based on some selected test cases. Both models employ the flexibility data generated by the NASTRAN, a finite element structural analysis program.⁸

Spacecraft Flexibility Model

The NASTRAN generated eigenvalues and eigenvectors of the flexible body are used for deriving information about the "transfer functions" of the spacecraft structure. The generated data contains the modal frequencies along with the coefficient for each mode such that response can be generated at one point of the structure while another point is actuated. The transfer function containing N modes is the one given in Eq. (4).

The transfer function of interest for Galileo is between the SBA actuating point and the response at the scan platform. Recall from a previous section, the platform M axis would observe only the structural response along the stator Z axis when $\beta = 90 \text{ deg}$ and mostly along the stator X axis when $\beta = 170 \text{ deg}$. Flexibility data corresponding to these two cone angles have been selected for investigation. For each case, NASTRAN was used to generate modal data at selected spacecraft locations or grid points. Only the flexible modes below 15 Hz with dominant mode shapes are selected and used in the simulations. The modal frequencies, damping, and coefficients used for simulations are shown in Table 2.

NASTRAN generated flexibility data are truncated before use as input data for the DISCOS program. The process takes the "augmented body method" approach, which preserves the dynamic fidelity for DISCOS simulation while providing reasonable simulation cost.⁹ This process truncates some high-frequency modes, since they are usually not needed for a low-bandwidth (1 Hz) controller and are too expensive to be included in the computer simulations. This truncation process retains, however, those modes that will end up as the dominant low-frequency modes in the DISCOS simulation. Frequency response in the clock loop are shown in Fig. 2 for cone angle at 90 deg.

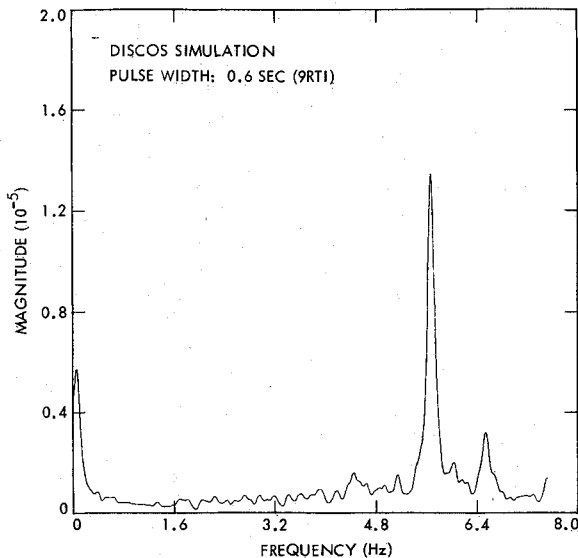


Fig. 6 Power spectral density of DISCOS generated vibrational data.

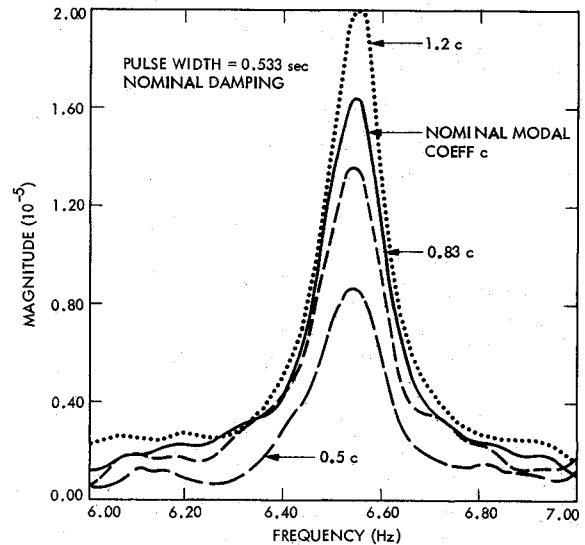


Fig. 8 Power spectral density vs modal coefficient.

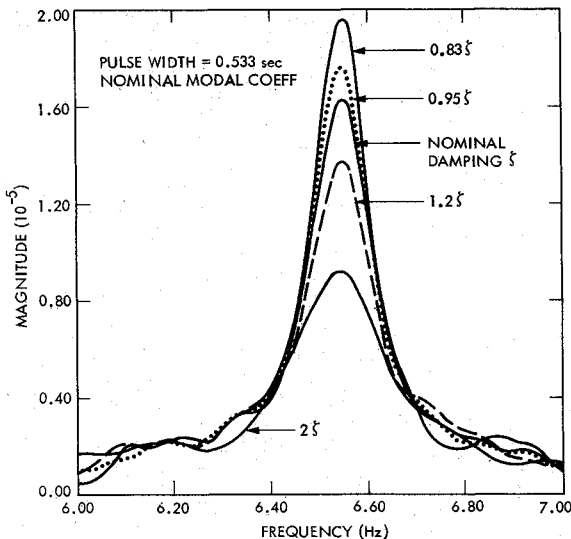


Fig. 7 Power spectral density vs damping.

Simulation Results

Torque response of the flexible stator at cone angle of 90 deg (i.e., scan platform M axis aligned with the stator Z axis) was simulated at pulse widths of 8, 9, and 10 RTI intervals. These responses are measured by gyros for 25 s at a 66⅔ ms sampling rate. A typical gyro measurement observed in telemetry is shown in Fig. 4. The corresponding PSD is shown in Fig. 5. The torque pulses were applied about the Z axis in the negative sense. The effective torque size is the difference between the torque saturation limit (4 N·m) and the slip ring friction (0.5 N·m, positive about Z) inherent to the clock actuator. As shown in the PSD, two dominant modal frequencies appeared at 5.69 Hz (alias of 9.31 Hz) and 6.57 Hz (alias of 8.43 Hz) with an accuracy of less than 3% error. The other four modes had small modal response and they appeared within the noise level of the PSD. The noise was contributed primarily by gyro quantization. The aliasing phenomenon is an effect of the gyro sampling rate (15 Hz). Any modal frequency above the Nyquist sampling frequency of 7.5 Hz (half of the sampling rate) will be aliased. It is sufficient to identify and notch out the aliased frequencies because they are the ones that will actually be observed by the scan controller.

The modal amplitude is proportional to the area underneath the "spike" curve on the PSD plot corresponding to each mode. Because different torque pulses contain different frequency harmonics, the same mode would have been excited differently, as determined by the level of the individual input power spectrum.

It is necessary to determine whether an identified frequency is actual or aliased for the modal parameter update. This can be easily deduced by correlating the PSD of both the torque input and the response output. No modal response should occur around a node of the input PSD. If verification is necessary, a torque pulse of a specified width can be sent in flight such that a node falls in one of the two possible resonance frequencies.

Figure 6 shows an example of the PSD derived from DISCOS-generated gyro measurements, using the same input (3.5 N·m for 9 RTI duration) as that in Fig. 5. The two PSD profiles are very similar and the frequencies and modal amplitudes have been determined to within the same level of accuracy. The slight discrepancy in the amplitude was probably due to dynamical cross couplings contained in the DISCOS simulation.

Once the resonance frequencies are determined, the damping factors and modal coefficients are then identified. Pulse width of 8 RTI (0.533 s) is selected for the 8.43 Hz mode because it can excite the mode to near its full amplitude. Figures 7 and 8 show the sensitivity of the PSD amplitude with respect to the damping and modal coefficient, respectively. Assume now that the PDS profile with nominal modal damping and coefficient corresponds to the profile generated from telemetry, i.e., the PSD that the model would try to match. Figure 7 shows that for a given modal coefficient, the matching of the PSD profile to that generated from telemetry data can be achieved by adjusting the damping. More importantly, this PSD profile has been shown to be quite sensitive to even a 5% change in damping. Note that for a constant modal coefficient, the base width of the amplitude remains constant while the height varies with damping. On the other hand, for a constant damping value as in Fig. 8, the area under the curve varies with the modal coefficient. These characteristics indicate the direction of adjusting the modal parameters in the model.

The shape of the PSD has demonstrated enough sensitivity to the modal parameters in Figs. 7 and 8 that once the PSD profile is reasonably matched, the modal damping and coefficient should be well within 10-20% accuracy. The only situation in which the PSD profile can be close to the nominal one

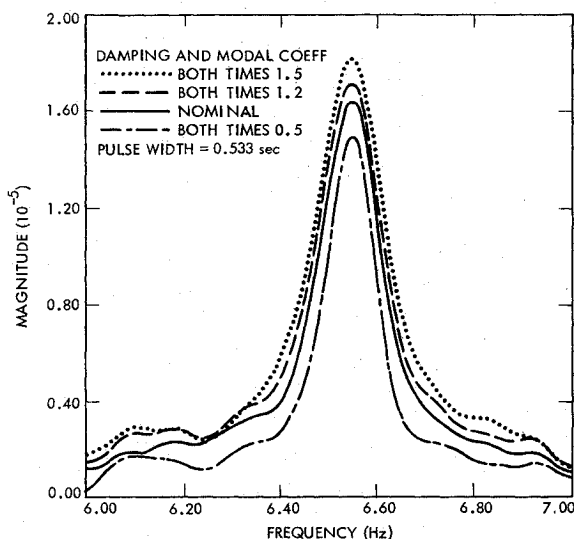


Fig. 9 Power spectral density vs change in damping and modal coefficient.

and yet have a large error is when both parameter estimates are simultaneously high or low. Nevertheless, in this case, there exists a family of curves that are still quite distinguishable from the nominal, as shown in Fig. 9. The shape of the PSD profile is still sufficiently sensitive to a 10-20% error in both estimates. In this case, both parameters can be respectively increased or decreased to keep the estimate error below 20%.

Conclusion

A scheme to identify the flexible mode characteristics (frequency, damping, and modal coefficient) of the Galileo stator structure using in-flight data has been presented. A frequency domain analysis approach is taken that involves generating a power spectral density of the structural response data based on the gyro measurements obtained from telemetry. The influence of the structural flexibility to the scan controller design has been explained and the constraints in executing the identification process in flight discussed.

A one-dimensional dynamics model containing the structural flexibility data has been used for computer simulation.

This model has further been verified by full-blown computer simulations of the spacecraft dynamics and platform controller using the Dynamic Interaction Simulation of Control and Structure (DISCOS) simulation program. Modal frequencies have been identified satisfactorily to within 3% error and modal damping and coefficient to within 20% error. Modal frequencies, coefficients, and damping are estimated for the purpose of updating the notch filter parameters in the scan platform controller. The flexible mode response not visible to the power spectral density would not cause instability as they should similarly be nonapparent to the scan controller.

Acknowledgments

The author would like to thank G. A. Macala for providing support in the NASTRAN/DISCOS models, J.L. Chodas for her effort in setting up the DISCOS simulation program, and W.G. Breckenridge and G.K. Man for their valuable advice and discussions. The research described in this paper was carried out at the Jet Propulsion Laboratory, California Institute of Technology, under contract with the National Aeronautics and Space Administration.

References

- ¹McGlinchey, L.F., "Planetary Spacecraft Pointing and Control—The Next 20 Years," American Astronautical Society, AAS Paper 80-017, Feb. 1980.
- ²Rasmussen, R.D. and Brown, T.K., "Attitude and Articulation Control Solutions for Project Galileo," American Astronautical Society, AAS Paper 80-109, Feb. 1980.
- ³Wong, E.C. and Lai, J.L., "In-Flight Identification of the Galileo Spacecraft Flexible Mode Characteristics," AIAA Paper 84-1965, Aug. 1984.
- ⁴Chodas, J.L. and Man, G.K., "Design of the Galileo Scan Platform Control," *Journal of Guidance, Control and Dynamics*, Vol. 7, p. 422, July-Aug. 1984.
- ⁵Dunn, H.J., "A Computer Program for Estimating the Power-Density Spectrum of Advanced Continuous Simulation Language Generated Time Histories," NASA TM 83120, June 1981.
- ⁶Papoulis, A., *Probability, Random Variables and Stochastic Processes*, McGraw-Hill Book Co., New York, 1965.
- ⁷Bodley, C.S., Devers, A.D., Park, A.C., and Frisch, H. P., "A Digital Computer Program for the Dynamic Interaction Simulation of Controls and Structure (DISCOS)," NASA TP 1219, May 1978.
- ⁸McCormack, C.W., *The NASTRAN Users' Manual*, NASA SP-222, Sept. 1970.
- ⁹Macala, G.A., "A Modal Reduction Method for Use with Nonlinear Simulations of Flexible Multibody Spacecraft," AIAA Paper 84-1989, Aug. 1984.